Spectrochimica Acta Part A 77 (2010) 630–637

Contents lists available at ScienceDirect

Spectrochimica Acta Part A: Molecular and Biomolecular Spectroscopy

journal homepage: www.elsevier.com/locate/saa

Synthesis, spectroscopic characterization and reactivity studies of oxovanadium(IV) complexes with bulky N,N′-polymethylenebis(3,5-^{t}Bu$_2$salicylaldimine) ligands

Veli T. Kasumov[a,*], F. Köksal[b], M. Aslanoglu[a], Y. Yerli[c]

[a] Department of Chemistry, Harran University, Osmanbey, 63300 Şanlıurfa, Turkey
[b] Department of Physics, Ondokuz Mayıs University, 55139 Kurupelit, Samsun, Turkey
[c] Department of Physics, Gebze Institute of Technology, Gebze-Kocaeli, Turkey

ARTICLE INFO

Article history:
Received 26 March 2010
Received in revised form 11 June 2010
Accepted 24 June 2010

Keywords:
[N,N′-polymethylenebis(3,5-^{t}Bu$_2$salicylaldimine)]VO(IV)
EPR
UV/vis
Chemical oxidation
Electrochemistry

ABSTRACT

A series of new sterically hindered N,N′-polymethylenebis(3,5-^{t}Bu$_2$salicylaldimine) ligands (H_2L_x) VO(IV) complexes, [VO{(2-O-3,5-^{t}Bu$_2$C$_6$H$_2$)CH=N-R-N=CH-(3,5-^{t}Bu$_2$-C$_6$H$_2$O-2)] (**X**), where R = $-(CH_2)_3-$ (**3**), $-(CH_2)_4-$ (**4**), $-(CH_2)_5-$ (**5**), $-(CH_2)_6-$ (**6**) and $-CH_2C(CH_3)_2CH_2-$ (**7**) and early reported $-(CH_2)_2-$ (**1**) and $-CH_2CH(CH_3)-$ (**2**), has been synthesized and characterized by spectroscopic (IR, UV/vis, ^{1}H NMR, EPR), electrochemical and magnetic susceptibility measurements. Complexes **1**–**7** are described a trigonal distorted pyramids. All seven compounds give nearly the same parallel hyperfine coupling constant (A_z) regardless that the geometry of VO(IV) changes from square pyramidal to trigonal distorted pyramids. Chemical oxidation of **1**–**7** by one equiv Ce(IV) leads to the formation of stable $[VO(V)L_x]^+$ complexes. Cyclic voltammograms of **2**–**6** in DMSO along with a quasi-reversible VO(IV)/VO(V) redox couple also showed irreversible phenolate/phenoxyl responses. Each **1** and **7** shows only one reversible VO(IV) centered oxidation waves. Chemical oxidation of H_2L_x forms the stable $[H_2L_x]^+$ radical species.

1. Introduction

The vanadyl ion ranks among the most stable of diatomic cations and dominates in the chemistry of vanadium. While the bulk of the vast literature relating to it dwells on synthetic, structural, spectroscopic, and magnetic aspects, the coordination chemistry of vanadium has recently become of great interest due to the presence of vanadium in enzymatic systems and catalytic activity [1,2]. Structural and functional models for vanadium-dependent enzymes, such as nitrogenases and haloperoxidases [2–4], and other vanadium containing biological molecules like amavadine [2e,g] have further stimulated research efforts on coordination chemistry [5–9]. Another important biological activity of vanadium is its insulin-mimetic characteristic, which can cause in vivo stimulation of the uptake and metabolism of glucose [4e,g]. The distinct preference of this metal center for O- and/or N-coordination environments has prompted the synthesis of numerous model vanadium compounds containing O/N donor ligands whose spectroscopic, magnetic, and redox properties have been widely investigated [3–8]. In addition, the ability to substitute vanadyl ion for spectroscopically silent divalent cations, such as Mg^{2+}, Ca^{2+}, and Zn^{2+} has led to the increased use of vanadyl ion (VO^{2+}), as a spectroscopic probe of biological systems using paramagnetic spectroscopic techniques, such as electron paramagnetic resonance (EPR), electron spin echo envelope modulation (ESEEM) and ENDOR [2d,5c]. These techniques can provide information such as the number, kinds and in some cases, orientations of ligands around the metal binding site. Tetradentate Schiff base–oxovanadium(IV) complexes along with a rich redox chemistry also exhibit catalytic activity in asymmetric oxidation of sulfides into the corresponding sulfoxides, selective epoxidation of olefins and C–C coupling reactions of various organic compounds [6d,8e].

This work is based upon our ongoing interest [9c,d] in the coordination chemistry of the redox-active di-tert-butylated sterically hindered phenol functionalized ligands transition metal complexes. One of the unique properties of above complexes is that they easily generate peripherally bonded stable M(II)-phenoxyl radical complexes upon chemical oxidation [9]. The widespread occurrence of tyrosine radicals [10] in metalloproteins involving oxygen-dependent enzymatic radical catalysis has prompted inorganic chemists to model tyrosine by using di-tert-butylphenolate ligands [10,11]. In our previous reports [12,13], we have demonstrated that some Cu(II), Co(II) and Pd(II) complexes with bidentate N-aryl(alkyl)-3,5-^{t}Bu$_2$salicylaldimines and tetradentate N,N′-bis(3,5-^{t}Bu$_2$-salicylidene)-polymethylenediamine type

---

[*] Corresponding author. Tel.: +90 414 3283461 3588; fax: +90 414 3440051.
E-mail address: vkasumov@harran.edu.tr (V.T. Kasumov).

1386-1425/$ – see front matter © 2010 Elsevier B.V. All rights reserved.
doi:10.1016/j.saa.2010.06.040

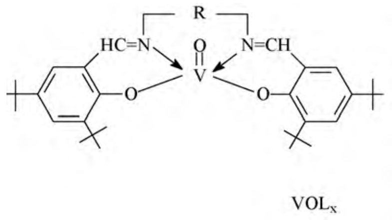

H_2L_x	VOL$_x$	R
H_2L_1	1	$-(CH_2)_2-$
H_2L_2	2	$-CH_2CH(CH_3)-$
H_2L_3	3	$-(CH_2)_3-$
H_2L_4	4	$-(CH_2)_4-$
H_2L_5	5	$-(CH_2)_5-$
H_2L_6	6	$-(CH_2)_6-$
H_2L_7	7	$-CH_2C(CH_3)_2CH_2-$

Scheme 1. Formula of the complexes.

ligands upon chemical oxidation affords directly coordinated phenoxyl radical complexes. Herein, we describe the synthesis, spectroscopic characterization, and chemical and electrochemical redox behaviors of a series of VO(IV) chelates (VOL$_x$, abbreviated as **1**–**7**) with tetradentate N,N′-bis(3,5-^{t}Bu$_2$salicylidene)-polymethylenediamine ligands (H_2L_x) (Scheme 1).

2. Experimental

2.1. Measurements

All the methods of analysis [(C, H, N), FTIR, EPR, ^{1}H NMR] were carried out as described previously [12,13]. The ESR spectra were recorded on a Varian E-109 C model X-band spectrometer with 100 kHz frequency modulation. The *g*-values were determined by comparison with a $g = 2.0036$ of DPPH sample. The errors for *g* and *A* parameters are ±0.001 and ±0.005 G, respectively. The program SIMFONIA version 2.1 by Bruker was used for numerical simulation of the EPR spectra for an $S = 1/2$ electron spin coupled to the $I = 7/2$ nuclear spin from the ^{51}V nucleus. IR spectra obtained on a Perkin-Elmer FTIR spectrometer using KBr pellet. Electronic spectra were recorded by using a Perkin-Elmer Lambda 25 spectrophotometer in the 200–1100 nm region in $CHCl_3$, CH_3CN and DMF. The room temperature (r.t.) magnetic susceptibility was measured by using a Sherwood Scientific magnetic susceptibility balance. The diamagnetic corrections for ligand susceptibility were evaluated using Pascal's constants.

Chemical oxidation of **1**–**7** complexes (5×10^{-3}–3×10^{-2} M) was carried out by the addition of one or two molar equivalent $(NH_4)_2Ce(NO_3)_6$ [Ce(IV)] to their $CHCl_3$, CH_3CN, DMF or DMSO solutions at r.t. and under air conditions by using in situ UV–vis and EPR spectral measurements. UV–vis experiments were carried out in DMF or CH_3CN solutions of **X** by using equivalent molar Ce(IV). The observed spectral changes were monitored with a Perkin-Elmer Lambda 25 spectrophotometer. Electrochemical measurements were recorded at r.t. under a dry nitrogen using a PC-controlled Eco Chemie-Autolab-12 potentiostat in DMSO solutions of ca. 10^{-3} to 10^{-4} M of **X** containing 0.05 M n-Bu_4NClO_4 as the supporting electrolyte.

A conventional three-electrode configuration was used consisting of a Pt disc working and a Pt wire auxiliary electrodes and a Ag/AgCl reference electrode. Prior to each voltammetric experiment, oxygen free nitrogen was bubbled through the electrochemical cell to remove the oxygen for a few min. The potentials are referenced to Ag/AgCl in the +1.5 to −1.5 V potential range.

2.2. Materials

All chemicals and solvents were of reagent grade and were used without further purification. $VO(SO_4)\cdot5H_2O$, $(NH_4)_2Ce(NO_3)_6$ (ACN), 2,4-di-tert-butylphenol, all diamines, $NH_2-(CH_2)_n-NH_2$, where $n = 2$–6, 2-methyl-1,2-diaminoethane and 1,3-diamino-2,2-dimethyl-propane were obtained from Aldrich Chemical Co. The reagent 3,5-di-t-butylsalicylaldehyde was prepared from commercially available 2,4-di-tert-butylphenol according to the literature [14].

2.3. Synthesis of ligands

The synthesis and spectroscopic (^{1}H NMR, FTIR, UV–vis) characterization of the H_2L_x ligands except H_2L_7 were described early [8g,9c,10,13]. The ligand H_2L_7 was prepared by the condensation reaction between 1,3-diamino-2,2′-dimethylpropane and 3,5-di-tert-butyl-salicylaldehyde. Yield 88%, M.p. 181–183 °C, Anal. Calc. for $C_{35}H_{54}N_2O_2$ C, 78.60; H, 10.18; N, 5.23%. Found: C, 77.63; H, 9.92; N, 4.98%. IR (KBr pellet, ν [cm^{-1}]): 1632 (CH=N), 2860–2970 (C–H of $-CH_2-$ and ^{t}Bu). ^{1}H NMR (300 MHz; solvent $CDCl_3$; standard $SiMe_4$) δ: 13.91 (s, 2H, OH), 8.41 (s, 2H, HC=N), 7.43–7.44 (d. 2H, meta-coupled H in salicylic ring, $J = 2.67$ Hz), 7.15–7.16 (d, 2H, meta-coupled H in salicylic ring, $J = 2.67$ Hz), 1.51 [s, 18H, $C(CH_3)_3$], 1.35 [(s, 18H, $C(CH_3)_3$, 1.14 (s, 6H, CH_3))]. UV/vis (C_2H_5OH: λ ($\log\varepsilon$ M^{-1} cm^{-1})): 225(4.8), 231(sh), (4.1), 263(4.9), 331 (4.5), 414(2.36).

2.4. Synthesis of complexes

The complexes **1**, **2** and **7**, were prepared by the following procedures. The hot methanol (30 ml) solution of $VOSO_4\cdot5H_2O$ (0.5 mmol) was added to a deoxygenated hot mixture of Et_3N (1.0 mmol) and the ligand (0.5 mmol) dissolved in 50 ml of $CHCl_3$/MeOH (1:10 by volume). The mixture was heated to reflux with stirring for about 30–45 min under nitrogen. After reducing the volume to ca. 15 ml under nitrogen, reaction mixture allowed to stand at room temperature. The green precipitate was filtered and washed several times with water and methanol, and dried in the oven at ca. 50 °C. The complexes were recrystallized from chloroform-methanol mixture. Yield 85–92%. In our all attempts to prepare the **3**–**6** complexes by above procedure, a green precipitate that was collected by filtration and recrystallized from methanol/$CHCl_3$ mixture yield compounds which contain slightly amounts of insoluble part. Therefore, the **3**–**6** complexes were prepared as follows. To a hot deoxygenated methanol-acetone solution of ligand (0.005 mol) and sodium acetate trihydrate (0.01 mol) the oxovanadium(IV) sulfate pentahydrate (0.005 mol) in 1 ml water was added. The reaction mixture was heated under a dinitrogen atmosphere for 40–50 min. After reducing the volume to ca. 15–20 ml, the obtained olive green precipitate, collected by filtration, washed with water and methanol, and dried in the oven at ca. 70 °C. Yields: 71–77%. The **3**–**6** complexes prepared by this procedure are good soluble in $CHCl_3$, CH_3CN, DMSO and DMF. The complexes were characterized by IR, UV–vis and elemental analysis (C, H, N). Complexes: **3**: yield: 79%. M.p. 266–268 °C, elemental Anal.: calcd. for $C_{33}H_{48}N_2O_3V$ (571.69): C, 69.33; H, 8.46; N, 4.89%. Found: C, 69.62; H, 9.43; N, 4.47%. IR (KBr pellet, ν [cm^{-1}]): 1620 (CH=N), 2867–2957 (C–H of $-CH_2-$ and ^{t}Bu), new bands at 1536 and 1553 ((Ph-)C–C=N) bond, 978 (V=O). **4**: yield: 71%. M.p. dec. >270 °C. Calcd. for $C_{34}H_{50}N_2O_3V$ (585.71): C, 69.72; H, 8.60; N, 4.78%. Found: C, 69.52; H, 8.73; N, 5.57%. IR (KBr pellet, ν [cm^{-1}]): 1624 (CH=N), 2868-2955 (C–H of $-CH_2-$ and ^{t}Bu), new bands at 1542 and 1554 due to vibration of the (Ph–)C–C=N bond, 978 (V=O). **5**: yield: 77%. M.p. dec. >250 °C. Calcd. for $C_{35}H_{52}N_2O_3V$ (599.74): C, 70.08; H, 8.74; N, 4.67%. Found: C, 69.87; H, 8.63; N, 4.57%. IR (KBr pellet, ν [cm^{-1}]): 1626 (CH=N), 2866-2955 (C–H of $-CH_2-$ and ^{t}Bu), new bands at 1542 and 1554, 976 (V=O). **6**: yield: 74%. M.p. dec. >270 °C. Calcd. for $C_{36}H_{54}N_2O_3V$ (613.77): C, 70.44; H, 8.87; N, 4.56%. Found: C, 68.89; H, 6.81; N, 3.37%. IR (KBr pellet, ν [cm^{-1}]): 1625 (CH=N), 2868–2956 (C–H of $-CH_2-$ and ^{t}Bu), new bands at 1541 and 1554; 979 (V=O). **7**: yield: 92%. M.p. >295 °C. Calcd. for $C_{35}H_{52}N_2O_3V$ (599.74): C, 70.08; H, 8.74; N, 4.67%. Found: C, 70.27; H, 8.53; N, 4.27%. IR (KBr pellet, ν [cm^{-1}]): 1614 (CH=N),

Table 1
Electronic spectral data for **1**–**7** complexes.

Complex	μ_{eff} μ_B	Solvent	Electronic spectra λ_{max} (nm) (ε M^{-1} cm^{-1})
1	1.74	$CHCl_3$	388(12600), 500^s(100), 625(207), 850^s(31)
		DMF	377(9630), 400^s(4406), 490^s(64), 619(155), $660^{s(}$136), 820^s(30)
2	1.70	$CHCl_3$	387(24200), 420^s (11200), 500^4(59), 630(186)
		DMF	377(9889), 410^s(4730), 490^s(102), 622(144)
3	1.67	$CHCl_3$	329(8862), 382(7560), 530^s(46), 630^s(27), 865^s(18)
		DMF	358(1873), 541(52), 686^s(25), 846(15)
4	1.68	$CHCl_3$	381(6290), 400^s(2312), 540^s(71), 630^s(44), 900(10)
		DMF	329(7677), 317(5279), 420^s(2263), 530^s(41), 634(23), 852(11)
5	1.71	$CHCl_3$	360(3870), 400^s(1310), 535^s(69), 635^s(36), 914(8)
		DMF	339(7260), 350^s(7106), 540^s(62), 640^s(34), 856(22)
6	1.73	$CHCl_3$	356(6346), 400^s(2268), 540^s(74), 640^s(45), 864(15)
		DMF	340(6585), 353^s(2964), 532^s(48), 634(27), 852(30)
7	1.85	$CHCl_3$	385(11640), 430^s(2490), 490^s(140), 620^s(112), 63(124),
		DMF	378(6292), 420^s(1780), 490^s(113), 588(93), 660^s(86), 890^s(36)

^{s}Shoulder.

2869–2959 (C–H of $-CH_2-$ and ^tBu), new bands at 1542 and 1555, 984 (V=O).

3. Results and discussion

The complexes **1** and **2**, reported before [8d,13a], also were prepared for comparative studies of their oxidative behaviors. All **1**–**7** complexes are scarcely soluble in organic solvents except for $CHCl_3$, DMSO and DMF. Compounds **3**–**6** are soluble in all above solvents on a slight heating. Complexes **3**–**6** upon recrystallization from $CHCl_3$ particularly undergoes to the oxidation giving corresponding diamagnetic VO(V) compounds. All complexes are green color and their IR spectra exhibit strong band in the region 975–984 cm^{-1} due to ν(V=O) stretching suggesting their mononuclear nature [5,6].

3.1. IR

The spectroscopic characteristics and elemental analysis results of the H_2L_1–H_2L_6 ligands were reported in literature [13c,d]. The selected IR spectral data of H_2L_7 ligand and **3**–**7** complexes, along with their assignments, are given in Section 2. The ligands exhibit characteristic bands in regions 2860–2970, 2600–2700 and 1629–1634 cm^{-1} due to C–H of ^tBu and $(CH_2)_x$ groups, OH (intramolecular H-bands) and CH=N stretches, respectively. The bands of ν(CH=N) stretching (1629–1634 cm^{-1}) of H_2L_3–H_2L_7 undergoes shifts to lower frequencies by about of 6–16 cm^{-1} in the spectra of **3**–**7** (1614–1625 cm^{-1}), indicating coordination of the imine nitrogen. The IR spectra of HL_x free ligands exhibit a broad absorption band at ca. 2700 cm^{-1} due to ν(OH) involved in intramolecularly H-bonding that disappears upon complexation. These changes suggest that the ligands are coordinated via imine nitrogen and deprotonated OH group oxygen atoms to the VO(IV) center. The spectra of **X** unlike the free ligands also exhibit two new bands at ca. 1540 and 1550 cm^{-1} which may originate from the coupling between the C=C/C=N bonds and the aromatic ring [15]. The ν(V=O) stretching frequency is relatively insensitive to the square pyramidal-to-trigonal bipyramidal distortion. For complexes **3**–**7** the V=O frequencies are 978, 978, 976, 979 and 984 cm^{-1}, respectively, consistent with the terminal, non-bridged, oxo V=O bond [5,9]. In general, IR spectra of the salicylaldimine VO(IV) chelates show the ν(V=O) stretching band at about 980 cm^{-1} for a monomeric form and nearly at 860–880 cm^{-1} for a linear chin (V=O$\cdots$V=O$\cdots$) polymeric form [5c,d]. These findings indicate that all **1**–**7** complexes unlike their non-tert-butylated analogous do not exhibit polymeric structure with the formation of V=O$\cdots$V=O$\cdots$ chains [5c,d]. The intermolecular steric repulsions of di-t-butyl-substituents seem to prevent the formation of V=O$\cdots$V=O linkages.

3.2. Magnetic moments

The magnetic moment data of the **X** complexes are presented in Table 1. The oxovanadium(IV) complexes belong to S = 1/2 system and the magnetic moments for magnetically dilute mononuclear VO(IV) complexes would be very close to the spin-only magnetic moment of 1.73 BM, since the spin-orbit coupling constant (λ) is positive and the orbital contribution is almost completely quenched in VO(IV) complexes [5a,b]. The r.t. effective magnetic moments of **1**–**7** complexes are in the range 1.67–1.85 BM indicating the magnetically dilute nature of the complexes [5a,b]. The observed magnetic moment data for **1**–**6** complexes (Table 1), except **7** (1.84 BM) are close to the expected 1.73 BM and do not indicate any antiferromagnetic or ferromagnetic coupling of spins at room temperature [5]. These results suggest that there are no direct V–V interactions in the solid complexes. It is of interest that the μ_{eff} values of these complexes estimated from solid state and frozen glass EPR spectra were in the range of 1.71–1.75 BM and indicate the absence of magnetic exchange in solution.

3.3. Electronic spectral study

The electronic absorption spectral data obtained from spectra of **1**–**7** which recorded in $CHCl_3$ and DMF solutions are listed in Table 1. Representative visible spectra of **1**–**7** MF are given in Fig. 1. As can be seen from Table 1 and Fig. 1, the spectra of **3**–**7** complexes in non-coordinated $CHCl_3$ and coordinated DMF solutions exhibit three broad bands of low intensity (ε = 13–199 M^{-1}cm^{-1}) in 525–905 nm region. The spectra of **1** and **2** are nearly identical, except that the spectrum of **2** exhibits poorly distinguishable inflection around 830 nm (ε = 25 M^{-1} cm^{-1}) absorption, and that their spectra practically do not exhibit solvent dependent behavior. It is interesting that the visible spectra of **3**–**7** compounds are significantly different from those for **1** and **2** complexes. The visible spectra of **3**–**7** show three low intensity absorption bands in the 500–910 nm region at 525–564, 630–680 and 780–905 nm in $CHCl_3$ and at 490–550, 600–650, and 613–850 nm in DMF solutions (Table 1). These absorptions due to their low extinction coefficients (13–230 M^{-1} cm^{-1}) can be assigned (from lowest to highest energy) as the $^2B_2 \rightarrow {}^2E_\pi{}^*(d_{xy} \rightarrow d_{xz}, d_{yz})$ (I), $^2B_2 \rightarrow {}^2B_1 * (d_{xy} \rightarrow d_{x^2-y^2})$ (II), and $^2B_2 \rightarrow {}^2A_1 * (d_{xy} \rightarrow d_{z^2})$ (III) transitions, according to Ballhausen and Gray molecular orbital scheme [17]. Comparison of the visible absorptions of **3**–**7** complexes revealed that the low energy bands appeared in coordinating DMF solvent display a red shifts comparing to those in non-coordinating (or poorly coordinated) $CHCl_3$ solvent. The spectra of all **1**–**7** display higher intensity absorptions with $\varepsilon > 3 \times 10^3$ M^{-1} cm^{-1} in the 350–410 nm region,

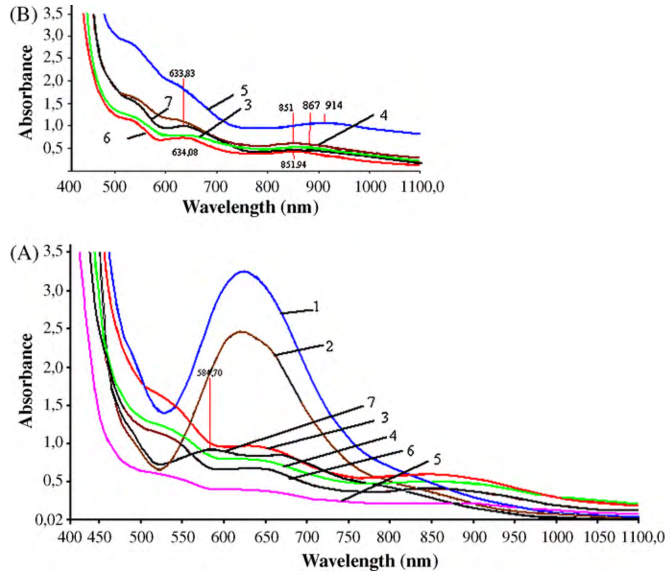

Fig. 1. (A) Electronic spectra of **1**–**7** complexes in DMF; (B) Electronic spectra of **3**–**6** complexes in $CHCl_3$ and **4** in DMF (**7**)

which could be assigned as ligand to metal charge transfer (LMCT), $p(\pi) \rightarrow d(\pi^*)$ transitions.

3.4. EPR spectra

Solid state EPR spectra. While the powder EPR spectra of **1** and **2** at r.t. exhibit a single broad isotropic signals with $g_{iso} = 1.983$ and 1.981, respectively, the solid state spectra of **3**–**7** display a broad structured features. Powder samples of **3** show structured EPR spectrum with $g_{av} = 1.985$. The spectra of solid **4** and **5** consist of five broad shoulders centered at ca. $g = 1.946$ and are more complicated for interpretation. At the same time, powder spectrum of **6** clearly displays structured symmetric feature centered at $g_{av} = 1.971$. However, the EPR spectra of all these solid samples recorded at 160 K do not exhibit any hyperfine structure and triplet state signal at ~1500 G due to the coupling of interacting ^{51}V nucleus. The appearance of the structured spectra for some VO(IV) complexes with longer $(CH_2)_x$ linkages ensure that in the polycrystalline state the VO(IV) centers are well spaced in the lattice diminishing mutual line broadening interactions [16a,17]. On the other hand, the possibility of the existence of various conformers in powder samples of these complexes [16b] also could complicate the solid state EPR spectra.

Solution EPR spectra. The r.t. isotropic EPR spectra of **1**–**7** complexes recorded in chloroform/toluene (V/V = 2:1) solution exhibit similar well resolved eight-line signals (Fig. 2) with $g_{iso} \sim 1.975–1.992 \pm 0.005$ and average hyperfine splitting A_{iso} of $86–92 \times 10^{-4}\,cm^{-1}$ (Table 2) resulting from coupling of the unpaired electron to the ^{51}V (I = 7/2, 99,75%; S = 1/2) nucleus. The EPR spectra of **1**–**7** recorded in $CHCl_3$/toluene solution at 160 K show well-resolved eight line axial anisotropy with two sets of eight line pattern with $g_{||} < g_{\perp}$ and $A_{\perp} \ll A_{||}$ relationships, characteristic of an axially compressed d^1_{xy} configuration [17–19]. The dipolar term $|A_{\perp} - A_{||}|$ remains approximately the same for all the complexes. This is consistent with the non-bonding nature of the electron-containing d_{xy} level [18a]. The possible superhyperfine couplings from ligand nitrogen or hydrogen nucleus on the vanadium lines are not observed. This indicates that the unpaired electron to be in a non-bonding b_{2g} (d_{xy}, $^2B_2$ ground state) orbital pointing away from the ligands in the equatorial (*xy*) plane and thus excluding the possibility of its direct interaction with the ligand [18,19]. The values of spin-Hamiltonian parameters extracted from simulated experimental frozen glass (160 K) EPR spectra of **1**–**7** are presented in Table 2. The simulation of the spectra was carried out by using the Bruker WINEPR Symfonia program. Representative experimental and simulated spectra of some complexes are shown in Fig. 3. The values of isotropic *g*-factors and hyperfine coupling constant, A_{iso}, were estimated as an average of the anisotropic *g* and *A* values calculated from simulated spectra [$A_{iso} = 1/3(A_z + A_x + A_y)$ and $g_{iso} = 1/3(g_z + g_x + g_y)$]. The spin-Hamiltonian parameters *A* and *g* are found to be in good agreement with those for analogous vanadyl complexes with square-pyramidal geometry [2d,7, and 8]. The r.t. and frozen glass spectra of **1**–**7** in $CHCl_3$ do not exhibit superhyperfine structure from ligands nitrogen or hydrogen atoms nucleus on the vanadium hyperfine line components. This indicates that the unpaired electron to be in b_{2g} ($3d_{xy}$, $^2B_2$ ground state) orbital localized on metal, thus excluding the possibility of its direct interaction with the ligand atoms [15,18]. The $A_{||}$ hyperfine coupling constant values ($158–164 \times 10^{-4}\,cm^{-1}$) (Table 2) for **X**, are in the range expected for complexes with the similar salicylaldimine ligands donor atoms [2,4–6]. As can be seen from Table 2 the difference $|A_{xx} - A_{yy}|$ generally increases with the number of $(-CH_2-)$ groups in **X**. For all complexes $|A_{xx}| < |A_{yy}|$ and $g_{yy} > g_{zz}$ were observed. Comparison of the in plain anisotropy indicates that both g_{xx} and g_{yy} are sensitive to changes in the structure. In addition, the obtained $A_{||}$ values are similar to the values calculated from additivity relationship described by Chasteen [1a] for VO(IV) com-

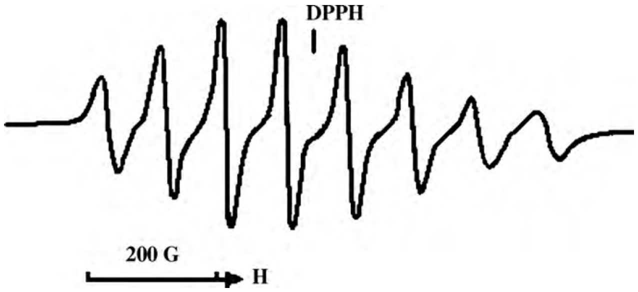

Fig. 2. EPR spectrum of **2** in $CHCl_3$ at r.t.

Table 2
The values of isotropic and anisotropic *g* and *A* components obtained from simulated frozen glass EPR spectra and calculated molecular orbital coefficients β_2^2 and α^2 for **1**–**7** compounds.

Complex **X**	g_{iso}[a]	A_{iso}[b]	g_{xx}	g_{yy}	g_{zz}	A_{xx}	A_{yy}	A_z	β_2^2	α^2
1	1.981	−88.3	1.989	1.985	1.970	−52.3	−54.2	−157.9	0.92	0.41
2	1.972	−89.8	1.983	1.980	1.955	−53.4	−55.6	−160.6	0.92	0.60
3	1.964	−86.9	1.978	1.965	1.949	−49.5	−52.8	−158.8	0.93	0.67
4	1.964	−91.6	1.979	1.974	1.940	−54.2	−57.0	−163.5	0.92	0.47
5	1.990	−86.1	1.997	1.973	1.945	−44.8	−54.2	−159.8	0.91	0.73
6	1.968	−88.4	1.990	1.971	1.945	−51.4	−55.1	−158.8	0.92	0.71
7	1.977	−86.9	1.990	1.985	1.955	−49.5	−52.4	−159.8	0.93	0.60

[a] Estimated errors are ±0.001 for *g*-factors.
[b] Values for *A* are given in units of $10^{-4}\,cm^{-1}$ with estimated errors of $\pm 0.5 \times 10^{-4}\,cm^{-1}$.

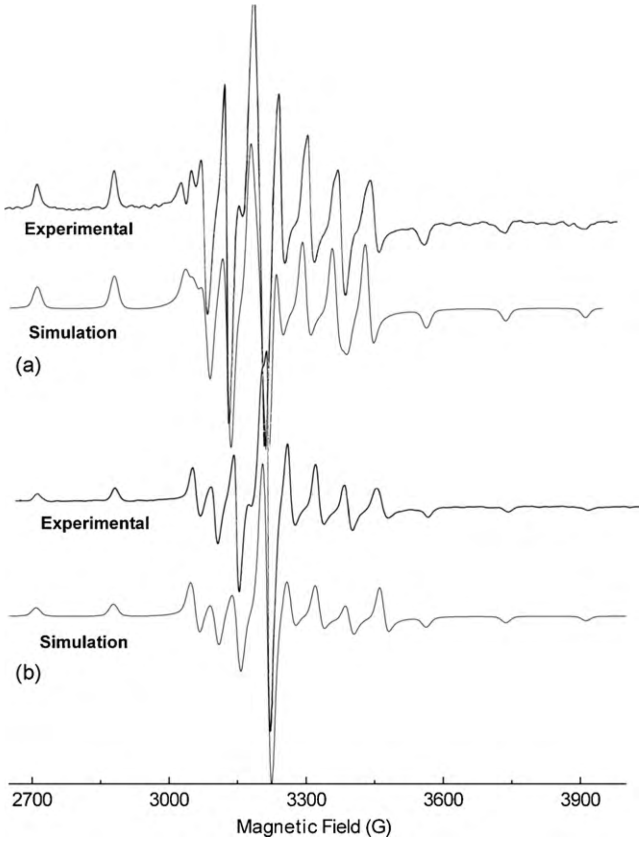

Fig. 3. Experimental and simulated EPR spectra of **2** and **4** complexes in $CHCl_3$ at 160 K.

plexes with ligands bearing two azomethine N and two phenolate O atoms in the coordination site [5–8]. Thus, the solution EPR spectra of **1**–**7** in $CHCl_3$ solution at 160 K are typical for square-pyramidal or distorted square-pyramidal geometries.

Molecular orbital theory is used to relate the measured principal components of **g** and **A** tensors to changes in the geometry and in the electronic structure of the vanadyl species. The relationship between the g and A hyperfine coupling constant and bond covalency has been studied by Kivelson Lee and McGarvey [18]. The principal components of the hyperfine tensor are given by the approximate relationships of (1)–(4). The squared MO coefficient β_2^2 can be determined from a suitable linear combination of (1) and (2) according to Eq. (3). Using the obtained values of β_2^2, $\lambda = 170\,\text{cm}^{-1}$ and $\Delta E_{x^2-y^2} = E_{x^2-y^2} - Ed_{xy}$, in-plane σ-bonding α^2 was estimated from Eq. (4)

$$A_{||} = -P_d\left[\left(K + \frac{4}{7}\right)\beta_2^2 + \Delta g_{||} + \left(\frac{3}{7}\right)\Delta g_{\perp}\right] \tag{1}$$

$$A_{\perp} = -P_d\left[\left(K - \frac{4}{7}\right)\beta_2^2 + \left(\frac{11}{14}\right)\Delta g_{\perp}\right] \tag{2}$$

$$\beta_2^2 = \frac{7}{6}\Delta g_{||} - \frac{5}{12}\Delta g_{\perp} - \frac{7}{6}\frac{A_{||} - A_{\perp}}{P_d} \tag{3}$$

$$\Delta g_{||} = \frac{8\lambda\alpha^2\beta_2^2}{\Delta E(^2B_2 \to {}^2B_1)} \tag{4}$$

where $P_d = 128 \times 10^{-4}\,\text{cm}^{-1}$ for VO(IV), $\Delta g_{||} = g_e - g_{||}$; $\Delta g_{\perp} = g_e - g_{\perp}$, K is Fermi contact term and related to the unpaired spin density at the nucleus [18b], α and β_2 are the coefficient of the vanadium $d_{x^2-y^2}$ and d_{xy} orbitals in the molecular orbital, respectively. Using the values of β_2^2, along with the observed energies for the electronic transitions $^2B_2 \to {}^2B_1$ appeared at around 600–650 nm and a spin-orbit coupling constant (λ) of 170 cm^{-1}, α^2 is calculated from Eq. (4). While the spectra yield only the magnitudes of $A_{||}$ and $A_{\perp}$, a negative sign of the hyperfine tensor components is required to obtain positive values for β_2^2 from Eq. (3).

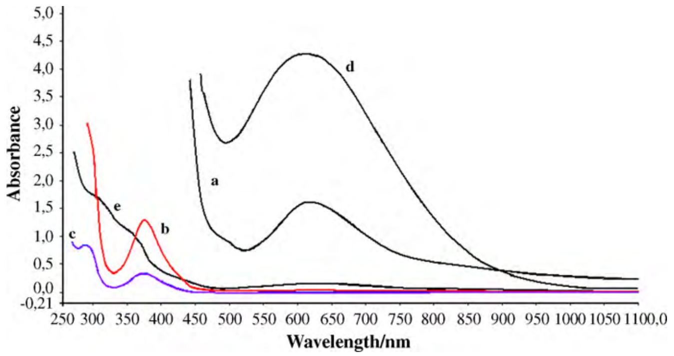

Fig. 4. Electronic spectra of **1** (a–c) and **1** + 1 equiv Ce(IV) (d) in DMF at r.t.; (e) spectrum of diluted (d).

The values of α^2 and β_2^2 calculated from Eqs. (4) and (3) for all **1**–**7** complexes are given in Table 2. The obtained values for β_2^2 (0.91–0.93) are close to the largest value of 1, which show that the in-plane π-bonding between d_{xy} orbital of VO(IV) and coordinating atoms is negligible. The quantity $C = 1 - \beta_2^2(0.07 - 0.09)$, which corresponds to the fraction of unpaired d-electrons that is delocalized over ligand orbitals, indicate that the unpaired electron in **1**–**7** practically localized in a $3d_{xy}$ orbital. The values for in plane σ-bonding parameter, α^2 (0.41–0.73) indicate that there is considerable σ-bonding covalency between VO(IV) and coordinating N/O atoms of the ligands in the **1**–**7** complexes.

*3.5. Chemical oxidation of **1**–**7***

Our recent studies on the chemical oxidation of bis[N-alkyl(aryl)-3,5-$Bu^t{}_2$-salicylaldi-minato]M(II) [M = Cu(II), Co(II), Pd(II)] complexes by $(NH_4)_2[Ce(NO_3)_6]$ [Ce(IV)] in $CHCl_3$ have revealed that the oxidation process was accompanied by the decrease of intensity of their EPR spectra [in the case of Cu(II) complexes] and appearance of the radical signals [12,13]. In the chemical oxidation of Co(II) complexes with di-tert-butylated bidentate, tridentate and tetradentate ligands unlike their non-di-tert-butylated analogues the generation of the stable Co(III)-phenoxyl radical complexes were detected in their EPR (octet of duplets at ca. $g = 2.00$).

The investigation of oxidative behavior of **1**–**7** complexes and H_2L_x ligands were carried out by using in situ UV-visible spectral measurements in CH_3CN and DMF. It has been found that upon addition of one molar equiv Ce(IV) to **1**–**7** in DMF at r.t., a simultaneous change of the light green to dark green blue, the disappearance of low intense d-d bands in the 600–850 nm region and appearance of new intense broad maximum band in the 592–780 nm were observed. In the oxidation of **1**–**7** complexes with one equiv molar Ce(IV) in DMF solution, along with instantly disappearance of original visible bands, the appearance of new absorptions with λ_{max}(ε, $M^{-1}\,cm^{-1}$) of 613 (1738), 612 (1265), 664(1918), 682 (780), 760 (213) and 780 (167) and 660 nm (1785), respectively, were detected (Figs. 4–6). As can be seen from Fig. 5 upon one-electron oxidation of **2**, along with the disappearance weak shoulder bands at ca. 800, 480 nm and UV bands 280 and 377 nm, the appearance of a new intense maximum band at 612 nm was detected. Similar spectral changes were also observed in CH_3CN. When the oxidation was carried out in CH_3CN the visible spectra of oxidized $\mathbf{1}^+$, $\mathbf{2}^+$, $\mathbf{3}^+$ and $\mathbf{6}^+$ species showed absorptions with λ_{max} (ε, $M^{-1}\,cm^{-1}$) of 615 (1300), 668 (1790), 663 (3090), and 660 (2090) nm, respectively,

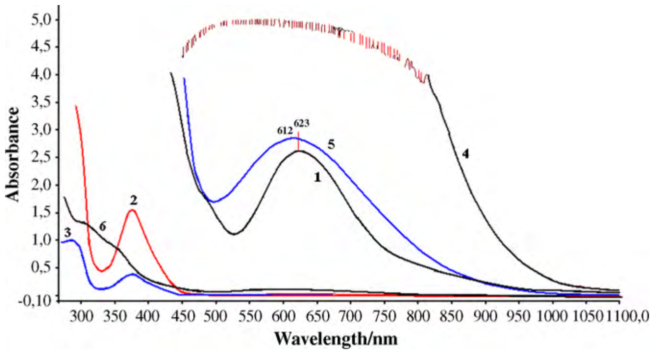

Fig. 5. Electronic spectra of **2** (0.016 M) and its oxidized species in DMF generated by the oxidation of one equiv molar Ce(IV) (0.016 M): (1), (2) and (3) spectra of **2** before the oxidation; spectra (4) just after oxidation and (5) after diluted 4 (3.2×10^{-3}); (6) spectrum of diluted 5.

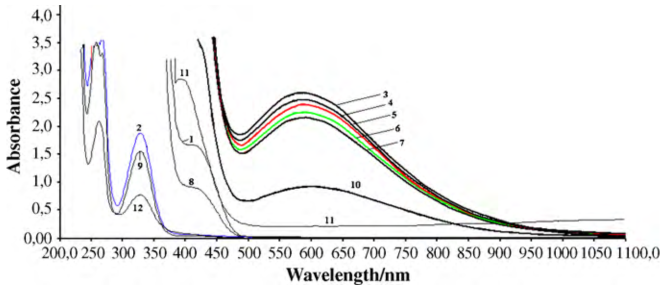

Fig. 7. Electronic spectra of some H_2L_x ligands and their one electron oxidation species generated by one equiv molar Ce(IV) in CH_3CN: (1) and (2) initial and dilute spectra of H_2L_1; (3)–(7) spectra of phenoxyl radical species scanned with 1 min intervals after oxidation of H_2L_1; (8) and (9) initial and dilute spectra of H_2L_2; (10) spectrum of phenoxyl generated from H_2L_2; (11) spectrum of phenoxyl radicals generated from H_2L_7; (12) spectrum of diluted (11).

but oxidized $\mathbf{4^+}$ and $\mathbf{5^+}$ exhibited absorptions with λ_{max} 592 (440) and 750 (sh, 303) nm, 662 (1496) and 780 nm(sh) in MeCN solution, respectively. It is of interest to note that upon addition of one equiv Ce(IV) to heterogeneous mixture of complexes **3**–**5** in MeCN, the insoluble part instantly dissolves and the reaction mixture becomes homogenous. The deep green blue colors of the oxidized $\mathbf{1^+}$–$\mathbf{7^+}$ species are presumably due to phenolate to oxovanadium(V) charge transfer transitions, and are comparable to other oxovanadium complexes of phenolate derived ligands [8]. When the course of oxidation process was monitored by EPR in CH_3CN, without detection of radical signals, the disappearance of VO(IV) EPR signal was observed. In the presented complexes one-electron oxidation process may be either metal-centered [$VO(IV)L_x \rightarrow VO(V)L_x$] or ligand-centered [$VO(IV)L_x \rightarrow VO(IV)L_x^{\bullet+}$] and in both cases the generated oxidized species should be diamagnetic (if antiferromagnetic coupling between d^1 and phenoxyl spins takes place for the latter one). While in both cases the generated $\mathbf{1^+}$–$\mathbf{7^+}$ species exhibit absorption bands in the 550–900 nm region, the visible absorptions in phenoxyl radicals originate from forbidden $n \rightarrow \pi^*$ transitions and appeared as low intensity bands ($\varepsilon = 100$–$500\,M^{-1}\,cm^{-1}$). In addition, phenoxyl radicals generally are unstable (under aerobic conditions they are rapidly decay) and also display typical strong absorption maxima around 350–400 nm and low intensity absorption at around 700–800 nm and $\lambda > 1100$ nm [9,10]. At the same time, the visible bands of VO(V) complexes originate from allowed LMCT transitions and exhibit high intensity absorptions ($\varepsilon = 1000$–$5000\,M^{-1}\,cm^{-1}$) and generally are stable under aerobic conditions. Since all of the spectra of oxidized **1**–**7** species did not exhibit absorption bands around 400 nm and display strong visible absorption bands in the 615–780 nm ($\varepsilon = 1300$–$3090\,M^{-1}\,cm^{-1}$) region and the oxidized species are stable under aerobic conditions it can be concluded that all these oxidation process is metal-centered and the oxidized species can be described as $[VO(V)L_x]^+$ cations. Thus, while the presented **1**–**7** complexes have two easily oxidizable metal centered VO(IV) and ligand centered 3,5-di-tert-butylphenolate group, the chemical oxidation takes place at the metal center.

Spectral change from light yellow to dark green or brownish orange also takes place upon oxidation of H_2L_x ligands under above conditions (Fig. 7). The oxidation of H_2L_2, H_2L_2 and H_2L_6 by one molar equiv Ce(IV) in CH_3CN, along with the simultaneous disappearance of original absorption at ca 410 nm and appearance of a new broad bands at 590(270), 600(186) and 704 nm, respectively, as well as absorption at $\lambda > 1100$ nm for $H_2L_5^{\bullet+}$, were observed. The appeared spectral patterns are typical for phenoxyl radical cations, $H_2L_x^{\bullet+}$ [10,21]. The generation of radical species was also supported by (the) detection of a single isotropic signal with $g = 2.005$ in the EPR spectra of the oxidized species in $CHCl_3$. In the oxidation of other H_2L_x ligands, the appeared green color instantly (for 4–5 s) converts to brownish orange and the detection of the absorbance of the generated species under above conditions were not possible. Thus, the presented experimental findings indicate that unlike Cu(II) and Co(II) complexes chemical oxidation of N,N′-polymethylenebis(3,5-^{t}Bu$_2$salicylaldimine)VO(IV) leads to the formation of [N, N′-polymethylenebis(3,5-^{t}Bu$_2$salicylaldimine)VO(V)]$^+$ complexes.

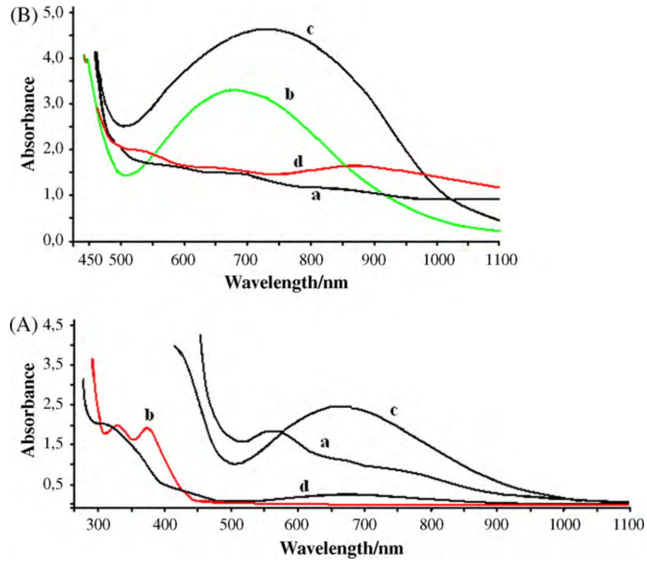

Fig. 6. Electronic spectra: (A) Visible spectra of **3** (a and b) and **3** + 1 equiv Ce(IV) (c and d) in DMF. (B) Spectra of **4** (a) and **4** + 1 equiv Ce(IV) (b) in DMF; spectra of **6** (c) and **6** + 1 equiv Ce(IV) in DMF recorded at r.t.

Table 3
Voltammetric data for **1**–**7** complexes.

Complex	E_{pa}^1	E_{pc}^1	ΔE_p	$E_{1/2}$	E_{pa}^2	E_{pc}^2
1	0.290	0.220	0.070	0.255	–	–
2	0.298	0.235	0.063	0.266	1.05	−0.442
3	0.376	0.247	0.129	0.312	0.95	−0.490
4	0.356	0.271	0.085	0.313	1.01	–
5	0.373	0.196	0.177	0.280	1.13	–
6	0.425	0.209	0.216	0,317	1.01	−0.459
7	0.319	0.250	0.069	0.285	–	–

Supporting electrolyte = 0.05 M n-Bu_4ClO_4, scan rate = 50 mV/s.
Potentials are presented in volts.
E^1 and E^2 represent the metal centered and ligand centered redox process, respectively.

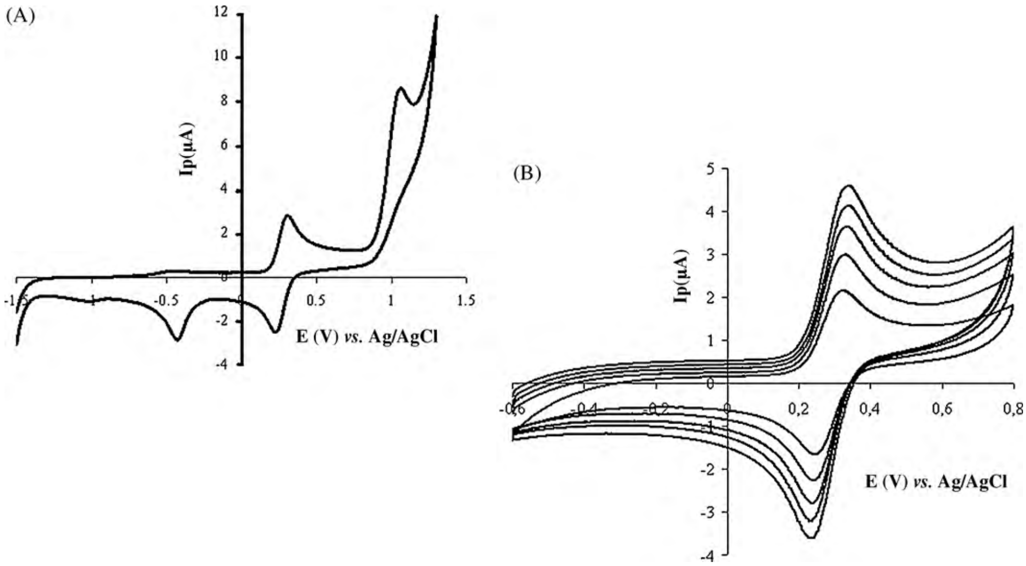

Fig. 8. (A) A cyclic voltammogram of complex **3** in DMSO and 0.05 M n-Bu_4NClO_4 as supporting electrolyte. Scan rate 50 mV/s. (B) Cyclic voltammograms of complex **7** in DMSO at increasing scan rates. Scan rates: 50, 100, 150, 200 and 250 mV/s.

3.6. Electrochemistry

The electrochemical behavior of **1**–**7** complexes were studied by cyclic voltammetry (CV) in the range +1.5 to −1.5 V in DMSO at Pt working electrode and Ag/AgCl reference electrode using n-Bu_4NClO_4 (0.05 M) as the supporting electrolyte. The results of cyclic voltammetry (CV) measurements are given in Table 3. Representative CV scans are shown in Fig. 8. The CV of **1**–**7** exhibit a quasi-reversible waves at $E_{1/2}$ of 0.266–0.317 and $\Delta E_p = 0.064$–0.216 V versus Ag/AgCl which can be ascribed to VO^{2+}/VO^{3+} oxidation couples (Table 3). The observed $E_{1/2}$ data for VO^{2+}/VO^{3+} waves are shifted to negative potentials comparing to those found for non-tert-butylated salen type VO(IV) complexes in DMF [6a] as expected for the greater σ electron donation of the tert-butyl groups attached to salicylic ring. The **1**, **2**, **4**, **7** and **3**, **5**, **6** complexes exhibit approximately reversible ($\Delta E_p = 0.063$–0.085 mV) and quasi-reversible ($\Delta E_p = 0.129$–0.216 V) processes, respectively, in DMSO at ca. 0.255–0.317 V versus Ag/AgCl due to VO^{3+}/VO^{2+} couple

$$\mathrm{VO(IV)} - \mathrm{e} = \mathrm{VO(V)} \tag{5}$$

The CV of **2**–**6** complexes also exhibit

$$\mathrm{VO(V)} = \mathrm{VO(IV)} + \mathrm{e} \tag{6}$$

The CV of **2**–**6** complexes also exhibit an irreversible anodic peak (Fig. 8a) in the potential range of +0.95 to +1.13 V (Table 3), which might be attributed to the one-electron oxidation of coordinating phenolates into phenoxyl radical species. The irreversibility of these curves suggests the instability of the generated radical species under electrochemical time scale. The CV of **2**, **3** and **6** display an irreversible peaks at −0.44, −0.49 and −0.46 V versus Ag/AgCl, respectively, which are absent in the CV of the free ligands, probably originate from products of the oxidized species. These reduction waves cannot be assigned to VO(IV)/VO(III), since the reduction potential of this couple is lower than −1.5 V in DMF [19,20]. The CV of **1** and **7** display only one reversible redox couple with $E_{1/2}$ at 0.255 and 0.285 V (Table 3), respectively. The quasi-reversibility of the complex **7** was also assured by the increase in peak current versus the square root of the scan rate as given in Fig. 8b. The $Ip/v^{1/2}$ value is almost constant for all scan rates. This establishes the electrode process as diffusion controlled [21]. It is interesting to note that the CV curves of all oxidized H_2L_x ligands in DMF, are similar to each other and exhibit only one irreversible wave in the range from +0.98 to 1.17 V versus Ag/AgCl [13c], indicating that the process accompanies O–H bond dissociation [22].

4. Conclusions

In conclusion, a series of sterically hindered salen complexes of VO(IV) with N,N′-polymethylenebis(3,5-$^{t}Bu_2$salicylaldimine) ligands have been prepared and characterized spectroscopically, magnetochemically and electrochemically. The bonding coefficients α^2 and β_2^2 were evaluated from the available MO theory and experimental UV/vis and EPR data. The presented complexes unlike their non-di-tert-butylated analogues did not form polymeric structure in solid state and adopted particularly trigonal distorted square-pyramidal geometry in $CHCl_3$ solution. It was also shown that the chemical oxidation of all complexes without generation of phenoxyl radical species readily forms corresponding stable $[VO(V)L_x]^+$ complexes. Cyclic voltammograms of **1**–**7** along with a quasi-reversible VO(IV)/VO(V) redox couples also showed irreversible oxidation waves assigned to phenolate/phenoxyl responses.

Acknowledgment

Financial support by the Harran University Research Grants Council is gratefully acknowledged.

References

[1] (a) N.D. Chasteen, in: L.J. Berliner, J. Reuben (Eds.), Biological Magnetic Resonance, Plenum Press, New York, 1981;
(b) S.W. Taylor, B. Kammerer, E. Bayer, Chem. Rev. 97 (1997) 333;
(c) A. Butler, C.J. Carrano, Coord. Chem. Rev. 109 (1991) 61;
(d) C. Bolm, Coord. Chem. Rev. 237 (2003) 245.
[2] (a) H. Vilter, Phytochemistry 23 (1984) 1387;
(b) R.L. Robson, R.R. Eady, T.H. Richrdson, R.W. Miller, M. Hawkins, J.R. Postgate, Nature 322 (1986) 388;
(c) D. Rehter, Coord. Chem. Rev. 182 (1999) 297;
(d) T.S. Smith, R. LoBrutto, V.L. Pecoraro, Coord. Chem. Rev. 228 (2002) 1–18;
(e) F.E. Mabbs, Chem. Soc. Rev. 22 (1993) 313;
(g) M. Helliwell, C.D. Garner, Angew. Chem. Int. Ed. 38 (1999) 795.
[3] (a) H.S. Soedjak, A. Butler, Inorg. Chem. 29 (1990) 5015;
(b) D.C. Crans, R.A. Felty, M.M. Miller, J. Am. Chem. Soc. 113 (1991) 265;
(c) R. Wever, E. De Boer, B.E. Krenn, H. Plat, H. Offenberg, Prog. Clin. Biol. Res. 274 (1988) 477;

(d) A.G. Ligtenbarg, R. Hage, B. Feringa, Coord. Chem. Rev. 237 (2003) 89;
(e) T. Kiss, T. Jakusch, J.C. Pessoa, I. Tomaz, Coord. Chem. Rev. 237 (2003) 123.

[4] (a) K.H. Thompson, J.H. McNeill, C. Orving, Chem. Rev. 991 (1999) 2561;
(b) A. Shisheva, Y. Shechter, J. Biol. Chem. 268 (1993) 6463;
(c) J. Li, G. Elberg, D.C. Garns, Y. Shechter, Biochemistry 35 (1996) 8314;
(d) E. Tsuchda, K. Oyaizu, Coord. Chem. Rev. 237 (2003) 213;
(e) S.A. Dikanov, B.D. Liboiron, C. Orvig, J. Am. Chem. Soc. 124 (2002) 2969;
(g) K.H. Thompson, C. Orvig, Coord. Chem. Rev. 219–221 (2001) 1033.

[5] (a) J. Selbin, Coord. Chem. Rev. 1 (1966) 293;
(b) A. Syamal, Coord. Chem. Rev. 16 (1975) 309;
(c) R. Dinda, P. Sengupta, S. Ghosh, T.C.W. Mak, Inorg. Chem. 41 (2002) 1684;
(d) R.L. Farmer, F.L. Urbach, Inorg. Chem. 13 (1974) 587;
(e) G.A. Kolawole, K.S. Patel, J. Chem. Soc. Dalton Trans. (1981) 1241;
(g) C.R. Cornman, K.M. Geiser-Bush, S.P. Rowley, P.D. Boyle, Inorg. Chem. 36 (1997) 6401.

[6] (a) C.J. Chang, J.A. Labinger, H.B. Gray, Inorg. Chem. 36 (1997) 5927;
(b) A. Kumar, S.K. Das, J. Catal. 166 (1997) 108;
(c) E. Tsuchda, K. Oyaizu, E.L. Devi, F.C. Anson, Inorg. Chem. 38 (1999) 3704;
(d) P.P. Reddy, Ch.-Y. Chu, D.-R. Hwang, S.-K. Wang, B.J. Uang, Coord. Chem. Rev. 237 (2003) 257.

[7] (a) H. Mimoun, M. Mihnard, P. Brechot, L. Saussine, J. Am. Chem. Soc. 108 (1986) 3711;
(b) K.I. Smith, L.L. Borer, M.M. Olmstead, Inorg. Chem. 42 (2003) 7410;
(c) A. Jezierski, J.B. Raynor, J. Chem. Soc. Dalton Trans. (1981) 1.

[8] (a) J. Bonadies, C.J. Carrano, J. Am. Chem. Soc. 108 (1986) 4088;
(b) M.R. Maura, S. Khurana, C. Schulzke, D. Rehder, Eur. J. Inorg. Chem. (2001) 779;
(c) C.E. Hollway, M. Melnik, Rev. Inorg. Chem. 7 (1985) 75;
(d) Z. Liu, F.C. Anson, Inorg. Chem. 39 (2000) 274;
(e) M. Kojima, H. Taguchi, M. Tsuchimoto, K. Nakajima, Coord. Chem. Rev. 237 (2003) 183;
(g) D.A. Atwood, M. Harvey, J. Chem. Rev. 101 (2001) 37.

[9] (a) L. Sacconi, U. Campigly, Inorg. Chem. 5 (1966) 606;
(b) S. Yamada, Y. Kuge, Bull. Chem. Soc. Jpn. 42 (1969) 152;
(c) Y. Kuge, S. Yamada, Bull. Chem. Soc. Jpn. 42 (1969) 799;
(d) V.T. Kasumov, A.A. Medjidov, Koord. Khim. 17 (1987) 74;
(e) V.T. Kasumov, A.A. Medjidov, I.A. Golubeva, T.P. Vishnyakova, O.V. Şubina, R.Z. Rzaev, Russ. J. Coord. Chem. 17 (1991) 1698.

[10] (a) P. Chaudhuri, M. Hess, U. Flörke, K. Wieghardt, Angew. Chem. Int. Ed. 37 (1998) 2217;
(b) P. Chaudhuri, M. Hess, T. Weyhermüller, K. Wieghardt, Angew. Chem. Int. Ed. 38 (1999) 1095;
(c) P. Chaudhuri, M. Hess, J. Müller, K. Hildebrand, E. Bill, T. Weyhermüller, K. Wieghardt, J. Am. Chem. Soc. 121 (1999) 9599;
(d) J.-L. Pierre, Chem. Soc. Rev. 29 (2000) 251;
(e) B.A. Jazdewski, W.B. Tolman, Coord. Chem. Rev. 200–202 (2000) 833.

[11] (a) N. Ito, S.E.V. Philips, C. Stevens, Z.B. Orgel, M.J. McOherson, J.N. Keen, K.D.S. Yadav, O.J. Knowles, Nature 350 (1991) 87;
(b) J. Stubbe, W.A.V. der, Donk, Chem. Rev. 98 (1998) 705;
(c) C.W. Wittaker, Chem. Rev. 103 (2003) 2347;
(d) F. Thomas, G. Gellon, I. Gautier-Luneau, E. Saint-Aman, J.-L. Pierre, Angew. Chem. Int. Ed. 41 (2002) 3047;
(e) L. Benisvy, A.J. Blake, D. Collison, G. Whittaker, C. Wilson, J. Chem. Soc. Dalton Trans. (2003) 1975.

[12] (a) V.T. Kasumov, F. Köksal, R. Köseoğlu, J. Coord. Chem. 57 (2004) 591;
(b) V.T. Kasumov, F. Köksal, A. Sezer, Polyhedron 24 (2005) 1203;
(c) V.T. Kasumov, A.I. Öztürk, F. Köksal, Polyhedron 26 (2007) 3129.

[13] (a) V.T. Kasumov, I. Ucar, A. Bulut, J. Fluorine Chem. 131 (2010) 59;
(b) V.T. Kasumov, F. Köksal, Spectrochim. Acta A 61 (2005) 225;
(c) Ş. Özalp-Yaman, V.T. Kasumov, A.M. Önal, Polyhedron 24 (2005) 1821;
(d) V.T. Kasumov, Ş.Ö. Yaman, E. Taş, Spectrochim. Acta A 62 (2005) 716.

[14] J.F. Larrow, E.N. Jacobsen, Y. Gao, Y. Hong, C.M. Zeppe, J. Org. Chem. 59 (1994) 193.

[15] (a) S.J. Gruber, C.M. Harris, E. Sinn, J. Inorg. Nucl. Chem. 30 (1968) 1805;
(b) J.W. Leadbetter Jr., J. Phys. Chem. 81 (1977) 54;
(c) I. Cavaco, J.C. Pessoa, M.T. Duarte, R.T. Henriques, P.M. Matias, R.D. Gillard, J. Chem. Soc. Dalton Trans. (1996) 1989.

[16] (a) S. Mondal, P. Ghosh, A. Chakravorty, Inorg. Chem. 36 (1997) 59;
(b) K. Ramaiah, F.E. Anderson, D.F. Martin, Inorg. Chem. 3 (1964) 298.

[17] C.J. Ballhausen, H.B. Gray, Inorg. Chem. 1 (1962) 111.

[18] (a) D. Kivelson, S.K. Lee, J. Chem. Phys. 4 (1964) 1896;
(b) B.R. McGarvey, J. Phys. Chem. 71 (1967) 51;
(c) K.P. Callahan, P.J. Durand, Inorg. Chem. 19 (1980) 3211.

[19] G.R. Hausan, T.A. Kabanos, A.D. Keramidas, D. Mentazafos, A. Terzis, Inorg. Chem. 31 (1992) 2587.

[20] (a) N.F. Choudhary, N.G. Connelly, P.B. Hitchcock, G.J. Leigh, J. Chem. Soc. Dalton Trans. (1999) 4437;
(b) J.C. Dutton, G. Fallon, K.S. Murray, Inorg. Chem. 27 (1988) 34.

[21] J. Losada, I. del Peso, L. Beyer, Inorg. Chim. Acta 321 (2001) 107.

[22] (a) F. Tomas, O. Jarjayes, C. Duboc, J. Philouze, E.S. Aman, J.L. Pierre, J. Chem. Soc. Dalton Trans. (2004) 2662;
(b) F.G. Bordwell, J.P. Cheng, J. Am. Chem. Soc. 113 (1991) 1736.